STEM CELLS AND DEVELOPMENT
Volume 30, Number 2, 2021

DOI: 10.1089/scd.2020.0162

BMP Ligand Trap ALK3-Fc Attenuates Osteogenesis and Heterotopic Ossification in Blast-Related Lower Extremity Trauma

Amy L. Strong,[1,*] Philip J. Spreadborough,[2,3,*] Devaveena Dey,[2,3] Peiran Yang,[4] Shuli Li,[1] Arthur Lee,[5] Ryan M. Haskins,[2] Patrick D. Grimm,[2,3] Ravi Kumar,[6] Matthew J. Bradley,[2,3] Paul B. Yu,[4] Benjamin Levi,[1,7] and Thomas A. Davis[2,3]

Traumatic heterotopic ossification (tHO) commonly develops in wounded service members who sustain high-energy and blast-related traumatic amputations. Currently, no safe and effective preventive measures have been identified for this patient population. Bone morphogenetic protein (BMP) signaling blockade has previously been shown to reduce ectopic bone formation in genetic models of HO. In this study, we demonstrate the efficacy of small-molecule inhibition with LDN193189 (ALK2/ALK3 inhibition), LDN212854 (ALK2-biased inhibition), and BMP ligand trap ALK3-Fc at inhibiting early and late osteogenic differentiation of tissue-resident mesenchymal progenitor cells (MPCs) harvested from mice subjected to burn/tenotomy, a well-characterized trauma-induced model of HO. Using an established rat tHO model of blast-related extremity trauma and methicillin-resistant *Staphylococcus aureus* infection, a significant decrease in ectopic bone volume was observed by micro-computed tomography imaging following treatment with LDN193189, LDN212854, and ALK3-Fc. The efficacy of LDN193189 and LDN212854 in this model was associated with weight loss (17%–19%) within the first two postoperative weeks, and in the case of LDN193189, delayed wound healing and metastatic infection was observed, while ALK3-Fc was well tolerated. At day 14 following injury, RNA-Seq and quantitative reverse transcriptase–polymerase chain reaction analysis revealed that ALK3-Fc enhanced the expression of skeletal muscle structural genes and myogenic transcriptional factors while inhibiting the expression of inflammatory genes. Tissue-resident MPCs harvested from rats treated with ALK3-Fc exhibited reduced osteogenic differentiation, proliferation, and self-renewal capacity and diminished expression of genes associated with endochondral ossification and SMAD-dependent signaling pathways. Together, these results confirm the contribution of BMP signaling in osteogenic differentiation and ectopic bone formation and that a selective ligand-trap approach such as ALK3-Fc may be an effective and tolerable prophylactic strategy for tHO.

Keywords: BMPRIA, ALK2/ALK3 kinase inhibitors, bone morphogenic protein (BMP), heterotopic ossification, trauma-induced extremity injury, limb amputation

Introduction

Aberrant wound healing following musculoskeletal polytrauma can lead to traumatic heterotopic ossification (tHO) and is more common with high-energy blast-associated extremity injuries and with concomitant central nervous system (CNS) trauma [1]. The pathophysiology of tHO has been shown to form in ~60% of high-energy blast injury patients wounded during the recent efforts in Iraq and Afghanistan with varying degrees of severities [2,3]. Significant complications associated with tHO include chronic pain, impaired prosthetic fitting, decreased range of motion,

[1]Division of Plastic Surgery, Department of Surgery, University of Michigan Health Systems, Ann Arbor, Michigan, USA.
[2]Regenerative Medicine Department, Naval Medical Research Center, Silver Spring, Maryland, USA.
[3]Department of Surgery, Uniformed Services University of the Health Sciences, Bethesda, Maryland, USA.
[4]Division of Cardiovascular Medicine, Department of Medicine, Brigham and Women's Hospital, Harvard Medical School, Boston, Massachusetts, USA.
[5]National Center for Advancing Translational Sciences, National Institutes of Health, Rockville, Maryland, USA.
[6]Acceleron Pharma, Inc., Cambridge, Massachusetts, USA.
[7]Department of Surgery, University of Texas Southwestern Medical Center, Dallas, Texas, USA.
*These authors contributed equally to this work.

neurovascular compromise, and skin [4]. The underlying mechanism of ectopic bone formation in tHO is characterized by a robust influx of inflammatory cells and hypermetabolism that leads to dysregulation of normal tissue repair [5,6]. Specifically, myeloid cells are proposed to exert autocrine and paracrine effects on tissue-resident and/or recruited mesenchymal progenitor cells (MPCs) to aberrantly induce osteogenic differentiation [5,6].

Bone morphogenic protein (BMP) signaling has been associated with HO induction [7]. BMPs, belonging to the transforming growth factor-beta (TGF-β) superfamily, are known as pivotal regulators of embryogenesis, growth, and differentiation [8]. Several BMPs have been shown to promote osteogenesis through the osteogenic induction of MPCs [9]. The BMP ligands BMP-2, BMP-4, BMP-7, and BMP-9 are potent mediators of osteogenesis and play a central role in normal bone development and in HO formation [10,11]. BMP-2 in particular has been shown to induce the expression of osteocalcin, and transient expression of BMP-2 appears necessary and sufficient to induce bone formation [12]. Subsequent studies have shown that BMP-2 plays a critical role in chondrocyte proliferation and maturation during endochondral ossification [13]. Significant HO formation has been associated with increased BMP-2 expression in a mouse burn/tenotomy trauma injury model [14]. Inhibition of BMP-2, BMP-4, and BMP-7 signaling with a BMP ligand trap appears to reduce HO formation, further supporting the role of BMPs in aberrant bone formation [15]. In a mouse model of spinal cord injury-induced HO, the expression of BMP-2, BMP-4, BMP-7, and BMP-9 was increased and associated with enhanced HO formation [16]. BMP-7 induction has been shown to be associated with the increased expression of osteoblast differentiation markers, including alkaline phosphatase (ALP) and accelerated calcium mineralization [17,18]. Together, these findings demonstrate the importance of BMP ligands in both normal bone development and aberrant wound healing in the bone.

BMPs mediate their signaling activity by interacting with receptor complexes composed of type I (ALK1, ALK2, BMPRIA/ALK3, BMPRIB/ALK6) and type II TGF-β receptors (BMPRII, ACTRII, ACTRIIB) [19–21]. BMP receptors differentially modulate the responsiveness of target genes downstream of BMP2-mediated signaling. BMPRII and ACTRIIB are able to compensate for each other functionally in mediating BMP signaling [22]. Appendicular skeletal development is normal in mice expressing a conditional BMPRII knockout allele and the Prx1-Cre transgene, indicating that BMPRII is not required for limb development and loss of BMPRII is compensated by BMP signal transduction via other BMP receptors [23]. In cases of BMPRII deficiency, BMPs may recruit SMAD-dependent and SMAD-independent signaling to regulate and refine specific osteogenic inductive signals in osteoblasts and their precursors [24,25].

Given the limited efficacy of current therapeutic options in inhibiting tHO, pharmacological strategies for modulating BMP signaling have emerged as a promising strategy to inhibit ectopic bone formation. These strategies include small-molecule inhibitors and recombinant protein ligand traps [26]. In the current study, we targeted ALK2, ALK3, and several of their ligands including BMP2, BMP4, BMP6, and BMP7 to ascertain their roles in osteogenic differentiation and the efficacy of these molecules as potential therapies for HO in an established rat model of blast-related lower extremity trauma and methicillin-resistant *Staphylococcus aureus* (MRSA) infection. We found that the kinase inhibitors LDN193189 (which inhibits ALK2 and ALK3 preferentially) and LDN212854 (which exhibits biased inhibition of ALK2) and BMP ligand trap ALK3-Fc (which binds BMP-2 and BMP-4 most potently) reduced in vitro osteogenic differentiation of tissue-resident MPCs isolated from injured tissue following a burn/tenotomy insult [27–29]. LDN193189, LDN212854, and ALK3-Fc inhibited trauma-induced HO formation, with ALK3-Fc being well tolerated. Injured rats treated with ALK3-Fc demonstrated increased myogenic gene expression and decreased inflammatory gene expression. Consistent with these findings, ALK3-Fc treatment in vitro demonstrated reduced endochondral ossification, osteogenic differentiation, proliferation, self-renewal capacity, and alterations in gene expression of MPCs. Together, these results suggest that the BMP ligand trap ALK3-Fc may have promising therapeutic potential in limiting tHO formation and progression.

Materials and Methods

Animals

Adult wild-type C57BL/6 mice (*Mus musculus*) between 6 and 8 weeks old were purchased from Charles River Laboratory (Boston, MA). Mice were appropriately quarantined and allowed to acclimate in the vivarium at the University of Michigan, Ann Arbor, MI. All mice were housed in clean clear plastic cages and exposed to a 12-h light/dark cycle, with free access to standard rodent chow and water ad libitum, under veterinary care and supervision. All murine experiments and animal care procedures for this research were approved by the University of Michigan Institutional Animal and Care and Use Committee (IACUC). All activities were conducted in accordance with all applicable regulations and best practices pertaining to the use of animals in research.

Adult male Sprague Dawley rats (*Rattus norvegicus*) between 11 and 12 weeks old (350–450 g) were obtained from Taconic Biosciences (Germantown, NY). Rats were appropriately quarantined and allowed to acclimate in the vivarium located at the Walter Reed Army Institute of Research (WRAIR, Silver Spring, MD). All rats were housed in clean clear plastic cages and exposed to a 12-h light/dark cycle, with free access to standard rodent chow and water ad libitum, under veterinary care and supervision. Rat weights were assessed before surgery and at various intervals during the study. All rat experiments and animal care procedures for this research were approved by the Naval Medical Research Center (NMRC) and WRAIR IACUC.

Small-molecule inhibitors and BMP ligand trap

LDN193189 and LDN212854 were synthesized as previously described [28,30]. The ligand trap ALK3-Fc, a recombinant ALK3 extracellular domain expressed as an immunoglobulin G Fc fusion protein, was provided by Acceleron Pharma through a Limited Purpose Cooperative Research and Development Agreement between Acceleron Pharma and NMRC.

Traumatic burn/tenotomy injury model, isolation and differentiation of murine MPCs, and inhibitor treatment

Wild-type C57BL/6 mice were subjected to the well-established burn/tenotomy injury model to induce HO, as previously described [31]. Briefly, mice received a 30% total body surface area partial-thickness burn on the shaved dorsum followed by left hind limb Achilles tendon transection, as previously described [31]. On postoperative day (POD) 7, murine tissue-resident mesenchymal progenitor cells (MPCs) were derived from tissue collected from the Achilles tendon injury site, as previously described [31]. Briefly, cells were separated via 70 μm cell strainer and digestive enzymes were quenched in standard growth medium [Dulbecco's modified Eagle's medium (DMEM) supplemented with 10% fetal bovine serum (FBS) and 1% penicillin/streptomycin]. Cells were spun down at 1,000 rpm for 5 min. The supernatant was discarded, and the cell pellet was subsequently expanded in standard growth media and split 1:3. All cells were used within one to four passages. To evaluate osteogenic differentiation of MPCs treated with kinase inhibitor or BMP ligand trap, MPCs were cultured in osteogenic differentiation medium (ODM) composed of DMEM, 10% FBS, 100 g/mL ascorbic acid, 10 mM glycerophosphate, and 1% penicillin/streptomycin and were treated with 750 nM of LDN193189, LDN212854, or ALK3-Fc for the duration of the study. Early osteogenic differentiation was assessed on day 6 by ALP staining and pixel quantification. Late osteogenic differentiation was assessed on day 12 by Alizarin red staining and quantified by pixel analysis, as previously described [15].

Trauma-induced blast and extremity injury and inhibitor administration

Rats were subjected to whole-body exposure to blast overpressure, femoral fracture, soft tissue quadriceps crush injury, and limb amputation through the zone of injury. Immediately following wound closure, three muscle sites immediately surrounding the amputation site were inoculated with MRSA (strain 107261; 1×10^6 colony-forming unit), as previously described [32]. For studies with the LDN inhibitors, rats were treated daily for 21 days starting POD1 with vehicle control (10 mM citrate buffer, pH 3.0), LDN-193189 (6 mg/kg), or LDN-212854 (6 mg/kg) via oral gavage. ALK3-Fc (3 mg/kg), dissolved in phosphate-buffered saline (PBS), was administered through intraperitoneal injections starting on POD1 twice weekly for a total of 28 days. Animal health status and body weights were recorded daily. Postoperatively, rats were monitored at least twice daily by animal care staff, research investigators, and veterinarians for animal activity, signs of pain, weight loss, wound dehiscence, or infectious tracts for the duration of the study. Wounds that exhibited signs of infection defined as drainage, progressive marginal erythema, or dehiscence were debrided. Rats were euthanized if they demonstrated signs of infection after a third debridement and/or extreme weight loss (>25%) during the first 3 weeks after injury.

Quantitative micro-computed tomography analysis

Total new bone formed at the site of amputation was quantified using a high-resolution micro-computed tomography (micro-CT) system (SkyScan 1176; Bruker microCT, Kontich, Belgium), and a standard phantom was used for normalization. Rats were imaged every 2 weeks with the final scan at postoperative week 12. Scans were performed using a 89-kV polychromatic X-ray beam, 256 μA current, and an exposure time of 81 ms per 180° rotation [33,34]. Images were processed using the NRecon Reconstruction software (Bruker) to align scan images and generate reconstructed three-dimensional and cross-sectional images. The volume of new ectopic bone was quantified using the Bruker micro-CT volumetric software version 1.14.10.0+, as previously described [32].

Histological analysis

Injured and contralateral limbs harvested at postoperative week 12 were fixed in 10% formalin for 1 week, followed by transfer to PBS. Formalin-fixed tissues were decalcified in 10% ethylenediaminetetraacetic acid (Sigma), paraffin embedded, and sectioned. Tissue sections were stained with hematoxylin and eosin (H&E; Richard-Allan Scientific, Thermo Scientific, Waltham, MA). After staining, slides were dehydrated in graded solutions of ethanol and Sub-X and then sealed with Permount Mounting Medium (Sigma). Images were acquired and quantified with the ScanScope CS2 (Aperio, Vista, CA) running Image Scope (Aperio).

Blood analysis for complete blood count and comprehensive metabolic profile

Tail vein blood collections were performed on naive, POD3-, POD7-, and POD14-treated rats in the ALK3-Fc group. Complete blood count (CBC) analysis was performed using a Sysmex XT-2000i Automated Hematology Analyzer (Sysmex America, Inc., Mundelein, IL). Comprehensive metabolic profile (CMP) was performed using a Vitros 350 Chemistry System (Ortho-Clinical Diagnostics, Raritan, NJ). CMP analysis encompassed a renal panel, electrolyte panel (sodium, potassium, carbon dioxide, chloride, urea nitrogen, creatinine), liver panel (aspartate aminotransferase, alanine aminotransferase, lactic acid dehydrogenase, ALP, bilirubin), metabolic panel (albumin, total protein, glucose, cholesterol, triglycerides), and creatine kinase levels. Samples were run on the same day and the remaining serum stored at −80°C before use.

Cell proliferation, analysis of ALP activity, and colony-forming unit assays of rat tissue-resident MPCs

Biopsies of skeletal muscle were aseptically harvested from the zone of injury in vehicle- and ALK3-Fc-treated rats on POD14, as previously described [32]. Briefly, samples (50–100 mg) devoid of fascia and fat were minced and incubated in a solution of 300 U/mL of collagenase type II (Worthington, Lakewood, NJ) for 2 h. A single-cell suspension was generated by consecutive straining through 70-μm followed by 40-μm nylon mesh cell strainers (BD BioSciences, San Jose, CA). Red blood cells were lysed by incubating filtered cells in ACK lysis buffer (Lonza, Walkersville, MD) for 5 min, followed by rinsing cells with ice-cold PBS. Cells were evaluated for their osteogenic differentiation potential. Cells were serially diluted and seeded in triplicates at a concentration of 1,000 cells per

well of a six-well plate in either regular mesenchymal stromal cell growth medium (DMEM-F12, supplemented with 10% FBS, 100 U/mL penicillin, and 100 μg of streptomycin; Lonza) or ODM (Lonza) and evaluated after 6 days. To evaluate cell proliferation, a bromodeoxyuridine (BrdU) cell proliferation assay was performed according to the manufacturer's instructions (Cell Signaling Technology). For quantification of cellular ALP activity (ALP assay; Sigma–Aldrich), cells were lysed in 150 μL of 1% Triton X-100 for 1–2 min, followed by the addition of an equal volume of *p*-nitrophenyl phosphate substrate for 1–2 min, and absorbance was read immediately at 405 nm. For colony-forming cell assays, plates were rinsed with PBS, followed by fixation with 100% methanol for 3–5 min, air-dried, stained with crystal violet for 2–3 min, and rinsed five times with tap water. Colonies derived from putative colony-forming progenitor (CFP) cell (>50 cells) populations were manually counted at 15× magnification using an inverted phase microscope.

RNA-Seq and analysis

On POD14, skeletal muscle tissue biopsies from the zone of injury surrounding the amputation site from rats treated with vehicle ($n=4$) or ALK3-Fc ($n=4$) were collected and stored in RNALater (Ambion, Inc., Austin, TX) at 4°C for 4 days before being removed and stored at −80°C. Total RNA was isolated using a TRIzol-based PureLink™ RNA Mini Kit (ThermoFisher Scientific) with DNase treatment. Library generation and sequencing were performed at the Genomics Platform at the Broad Institute (Cambridge, MA). An input of 10 ng total RNA was first purified using a 2.2× volume RNA-solid-phase reversible immobolization (SPRI) bead cleanup. The RNA was eluted into Mix #1 (containing 3′ RT primer, dNTP mix RNase inhibitor, and trehalose) to prime the samples for reverse transcription. Mix #2 (containing 5× Maxima RT buffer, Trehalose, $MgCl_2$, template-switching oligonucleotide (TSO), RNase inhibitor, and Maxima RNaseH-minus RT) was then added to facilitate both first- and second-strand cDNA synthesis. The samples were subjected to polymerase chain reaction (PCR) preamplification using Mix #3 (containing KAPA HiFi HotStart ReadyMix, ISPCR primer, and water) to amplify cDNA, followed by a 0.8× volume SPRI bead cleanup to purify PCR products. Concentration of cDNA was assessed using Quant-iT™ PicoGreen™ dsDNA Assay Kit (ThermoFisher Scientific) and adjusted to 0.25 ng/μL. cDNA libraries were constructed using a Nextera XT DNA Library Preparation Kit (Illumina). Tagmentation was performed to fragment the cDNA and add adapter sequences to the end of each fragment. After the tagmentation reaction was neutralized, libraries were PCR amplified using Illumina p7 and p5 index adapters. cDNA libraries were pooled and subjected to a final 0.9× volume SPRI bead cleanup. Library quality was assessed using a bioanalyzer trace, and final libraries have a size of 500 bp. Pooled libraries were adjusted to 2 nM and denatured using 0.1 N NaOH before sequencing. Flowcell cluster amplification and sequencing were performed according to the manufacturer's protocols using the NextSeq. Libraries were sequenced with a read structure of 2×38bp. Quality control and alignment of the sequenced reads, and principal component and differential expression analyses were performed using Array Studio V10.0 (OmicSoft; Qiagen). The paired reads were aligned to reference library Rat B6.0, gene model Ensembl.R94. Differential expression was assessed by comparing ALK3-Fc-treated versus untreated injured rat samples using DESeq2 [35]. Functional and pathway analyses were performed using g:Profiler [36] using lists of significantly upregulated and downregulated genes ordered by fold change.

RNA isolation and gene expression analysis of injured skeletal muscle

Biopsies of skeletal muscle were aseptically harvested from the zone of injury surrounding the amputation site in vehicle control ($n=4$) and ALK3-Fc-treated rats on POD3, POD7, and POD14 ($n=4$) to evaluate changes in gene expression related to chondrogenesis. RNA was stored in RNAlater (Ambion, Inc.) at 4°C for 4 days. Approximately 50 mg of muscle tissue was homogenized in 1 mL of QIAzol lysis reagent (Qiagen, Germantown, MD). RNA was extracted using RNeasy Lipid Tissue Mini kits (Qiagen) according to the manufacturer's instructions. Reverse transcriptase-PCR was used to convert 1 μg of RNA to cDNA. Selected mRNA transcripts for 83 genes consisting of chondrogenic, osteogenic, angiogenic, and cell matrix targets were examined by quantitative real-time PCR using a custom low-density microarray (Bio-Rad Laboratories). Cycle threshold (Ct) values per gene transcript were normalized to the endogenous housekeeping gene glyceraldehyde-3-phosphate dehydrogenase within each sample, and relative gene expression was calculated using the $2^{-\Delta\Delta Ct}$ method. A gene was reported as differentially regulated if there was greater than a two-fold difference in expression compared with naive controls. Altered genes were input into DAVID 6.8 [37] and Gene Ontology (GO) term, and Kyoto Encyclopedia of Genes and Genomes (KEGG) pathway analysis was performed.

Statistical analysis

All values are presented as mean ± standard error of the mean. The statistical differences between two or more groups were determined by analysis of variance, followed by post hoc Tukey multiple comparison tests. Statistical significance was set at $P<0.05$. Only statistically significant values were considered relevant. Analysis was performed using Prism 8.0 (GraphPad Software, San Diego, CA).

Results

ALK2/3 kinase inhibitors and BMP ligand trap reduces osteogenic differentiation

To evaluate the effects of ALK2/3 kinase inhibitors and a BMP ligand trap on osteogenic differentiation, murine tissue-resident MPCs were harvested following burn/tenotomy injury and treated with LDN193189, LDN212854, or ALK3-Fc in ODM. Significant reduction in osteogenic differentiation was evaluated by ALP staining following inhibitor treatment and ligand trap, and quantification of staining by densitometry revealed significant 2.7-fold reduction ($P<0.005$), 3.8-fold reduction ($P<0.001$), and 2.5-fold reduction ($P<0.005$) following treatment with LDN193189, LDN212854, and ALK3-Fc, respectively (Fig. 1A, B). Treatment with LDN193189, LDN212854, and

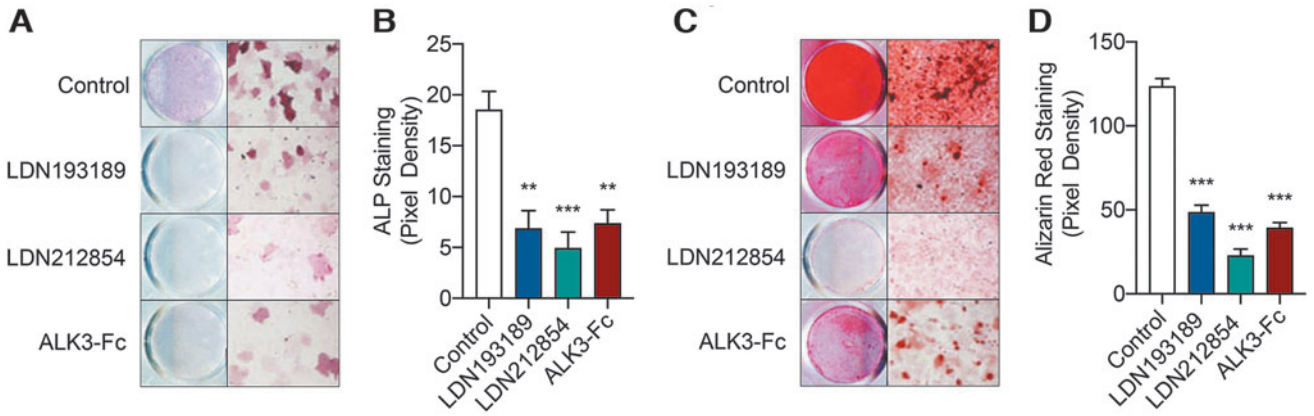

FIG. 1. BMP type I receptor kinase inhibitors limit early and late osteogenic differentiation of MPCs. Following burn/tenotomy injury, MPCs were harvested at the zone of injury on POD7 and cultured in ODM treated with LDN193189 (750 nM), LDN212854 (750 nM), or ALK3-Fc (750 nM). **(A)** Analysis of early osteogenic differentiation was performed by alkaline phosphatase staining following 6 days in ODM. **(B)** Pixel quantification of alkaline phosphatase staining. **(C)** Analysis of late osteogenic differentiation was performed by Alizarin red staining following 12 days in ODM. **(D)** Pixel quantification of alizarin red staining. Mean ± SEM. $^{**}P < 0.01$, $^{***}P < 0.001$, compared with vehicle treatment. SEM, standard error of the mean; ODM, osteogenic differentiation medium; BMP, bone morphogenetic protein; MPC, mesenchymal progenitor cell; POD, postoperative day.

ALK3-Fc significantly inhibited late osteogenic differentiation of tissue-resident MPCs as assessed by Alizarin red staining by 2.5-fold ($P < 0.0001$), 5.4-fold ($P < 0.0001$), and 31.4-fold ($P < 0.0001$), respectively (Fig. 1C, D). Taken together, the inhibition of osteogenic differentiation of MPCs by LDN193189, LDN212854, and ALK3-Fc in vitro suggests a requirement for BMP signaling in this process.

Targeting BMP inhibition and ligand signaling limits heterotopic ossification through reduced endochondral ossification in a rat model of blast-related extremity trauma and MRSA infection

To evaluate ectopic bone formation, a well-established rat model of blast-related extremity trauma and MRSA infection was utilized to evaluate the effects of LDN193189, LDN212854, and ALK3-Fc. Treatment with LDN193189 and LDN212854 resulted in substantial weight loss after injury in comparison to baseline values (Fig. 2A). LDN193189-treated rats had an 18.8% reduction in body weight at 2 weeks [$P < 0.02$ with no improvement at 3 weeks (−17.1%, $P < 0.05$)] post-amputation (Fig. 2A). Similarly, LDN212854-treated rats demonstrated reduced weights at 2 weeks (−18.6%; $P < 0.05$; Fig. 2A). Furthermore, some LDN193189-treated rats demonstrated signs of MRSA metastatic infection requiring early euthanization after 2 weeks of treatment ($n = 2$ of 8); one LDN212854-treated rat displayed signs of delayed wound healing ($n = 1$ of 8). LDN193189-treated ($n = 8$), LDN212854-treated ($n = 8$), and ALK3-Fc-treated ($n = 6$) rats demonstrated reduced ectopic bone formation from 48.5 mm^3 in vehicle control rats to 26.0 mm^3 ($P = 0.1296$), 21.7 mm^3 ($P < 0.005$), and 29.4 mm^3 ($P < 0.01$), respectively (Fig. 2B, C). No statistically significant difference was observed in ectopic bone volume between the LDN193189, LDN212854, or ALK3-Fc (Fig. 2B). However, given the significant adverse events associated with LDN193189 and LDN212854, further analyses were deferred with these kinase inhibitor probe molecules and performed with ALK3-Fc treatment only. Histological analysis with H&E staining of the residual femur at POD-84 was evaluated and showed some active zones of hypertrophic chondrogenesis and endochondral bone formation at the amputation site in the vehicle-treated animals at POD84, whereas ALK3-Fc-treated rats had a clearly demarcated fibrous capsule without signs of chondrogenesis (Fig. 2D). These results together suggest that ALK3-Fc is effective at suppressing tHO formation without the adverse effects noted with sustained LDN193189 and LDN212854 treatment in this blast and amputation with infection model.

Transient changes in blood cell counts associated with BMP ligand trap

To monitor the postoperative side effects of sustained ALK3-Fc treatment, blood was obtained from rats exposed to blast-related extremity injury for CBC and CMP measurements. CBC revealed no significant differences in white blood cell count on POD3, POD7, or POD14 (Fig. 3A) compared with vehicle-treated rats. ALK3-Fc treatment yielded a slight reduction in monocytes (from 0.8 K/μL in the vehicle-treated group to 0.4 K/μL in the ALK3-Fc-treated group, $P < 0.05$) on POD3 and slight increase in basophils (from 0.008 K/μL in the vehicle-treated group to 0.026 K/μL in the ALK3-Fc-treated group, $P < 0.05$) on POD7 (Fig. 3A). However, by POD14, there were no significant differences in either monocytes or basophils. While CMP analysis revealed mild differences in some serum chemistry values, these values were within the reference values. Creatinine kinase was the only value with significant reduction on POD14 (1141.7 U/L in vehicle-treated rats to 534.4 U/L in ALK3-Fc-treated rats, $P < 0.05$; Fig. 3B). Overall, no correlation was observed from serum chemistries on any day to suggest adverse renal, hepatic, cardiovascular, or musculoskeletal effects due to ALK3-Fc treatment.

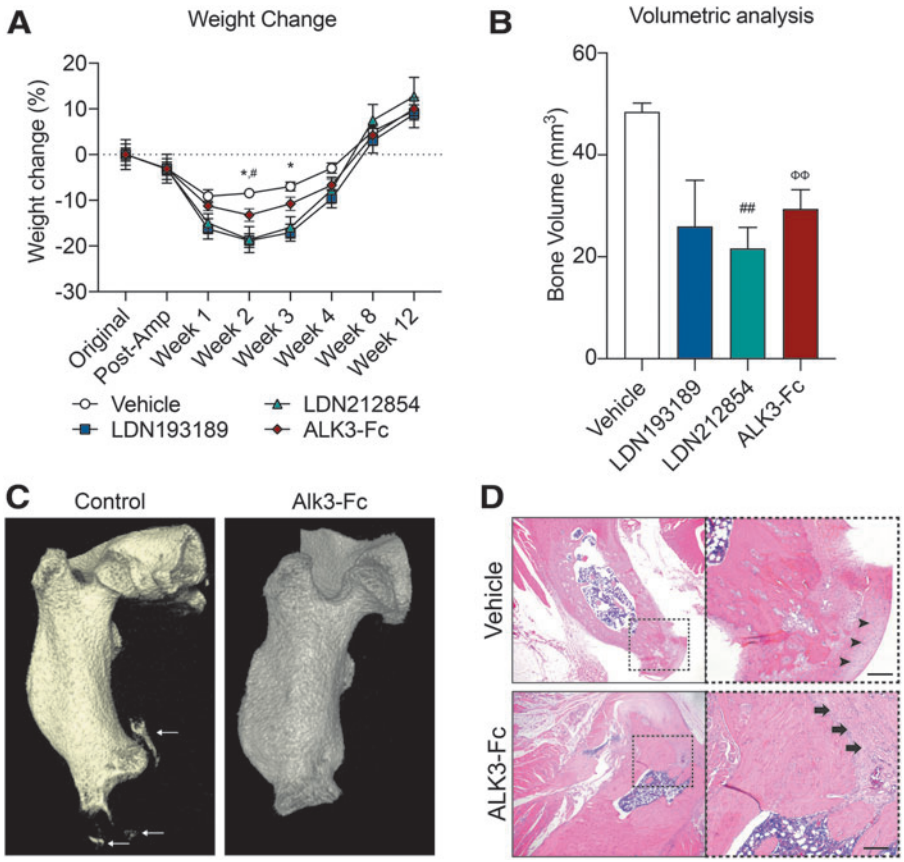

FIG. 2. BMP ligand trap ALK3-Fc limits endochondral ossification and heterotopic ossification and is well tolerated without any side effects. Rats were subjected to trauma that simulates a blast-induced extremity injury by exposing rats to blast overpressure, femur fracture, and a soft tissue crush injury, followed by an amputation through the zone of injury and then wound inoculation with MRSA following wound closure. Rats were then treated with vehicle (PBS, $n=6$), LDN193189 (oral lavage, 6 mg/kg daily for 21 days, $n=8$), LDN212854 (oral lavage, 6 mg/kg daily for 21 days, $n=8$), and ALK3-Fc (intraperitoneal injection, 3 mg/kg twice weekly for 28 days, $n=6$). **(A)** Animals were weighed every other week. **(B)** Micro-computed tomography scans were performed on animals following blast injury at 12 weeks. Total new bone was determined by defining the difference between new bone and naive bone. **(C)** Representative micro-computed tomography scan of rats treated with vehicle and ALK3-Fc at 12 weeks. *Arrows* highlight ectopic bone formation. **(D)** Representative hematoxylin and eosin images of sections in the ectopic bone region demonstrating the presence of fibrous capsule (*arrow*) around the amputation site without distinct chondrocytes (*arrowhead*) observed in the vehicle-treated control. Mean ± SEM. $^{*}P<0.05$, compared with vehicle- and LDN193189-treated rats; $^{\#}P<0.05$, $^{\#\#}P<0.01$, compared with vehicle- and LDN212854-treated rats; $^{\Phi\Phi}P<0.01$, compared with vehicle- and ALK3-Fc-treated rats. Scale bars, 20 μM. PBS, phosphate-buffered saline; MRSA, methicillin-resistant *Staphylococcus aureus.*

ALK3-Fc inhibits early osteogenic differentiation, proliferation, and self-renewal capacity of tissue-resident MPCs

To explore the effects of BMP ligand trap treatment on the osteogenic differentiation capacity of tissue-resident MPCs, tissue was harvested from the zone of injury surrounding the amputation site of vehicle- and ALK3-Fc-treated rats on POD14. Tissue-resident MPCs were evaluated for cell proliferation potential, CFP frequency, and early osteogenic differentiation capacity in both stromal media and ODM. Early osteogenic differentiation assessment by ALP demonstrated reduced osteogenic differentiation in ALK3-Fc-treated rats in both stromal media [0.12 absorbance units (AU) in vehicle-treated animals to 0.04 AU in ALK3-Fc-treated animals; 3.0-fold reduction; $P<0.0005$] and ODM (0.17 AU in vehicle-treated rats to 0.03 AU in ALK3-Fc-treated rats; 5.6-fold reduction; $P<0.01$; Fig. 4A). The tissue-resident MPCs isolated from ALK3-Fc-treated rats were assessed by BrdU staining and demonstrated reduced proliferation in stromal media from 1.21 AU in vehicle-treated rats to 0.27 AU in ALK3-Fc-treated rats (4.5-fold reduction; $P<0.05$) and in ODM from 0.94 AU in vehicle-treated rats to 0.16 AU in ALK3-Fc-treated rats (5.9-fold reduction; $P<0.002$; Fig. 4B). Quantification of tissue-resident MPCs revealed a significant reduction in CFPs in stromal media (78.8 ± 9.0 CFPs in vehicle-treated rats to 36.2 ± 6.6 CFPs in ALK3-Fc-treated rats; $P<0.02$) and ODM (48.6 ± 6.5 CFPs in vehicle-treated rats to 0.3 ± 0.16 CFPs in ALK3-Fc-treated rats; $P<0.002$; Fig. 4C). Together, these results suggested that treatment with ALK3-Fc reduces osteogenic differentiation, proliferation, and self-renewal capacity of tissue-resident MPCs.

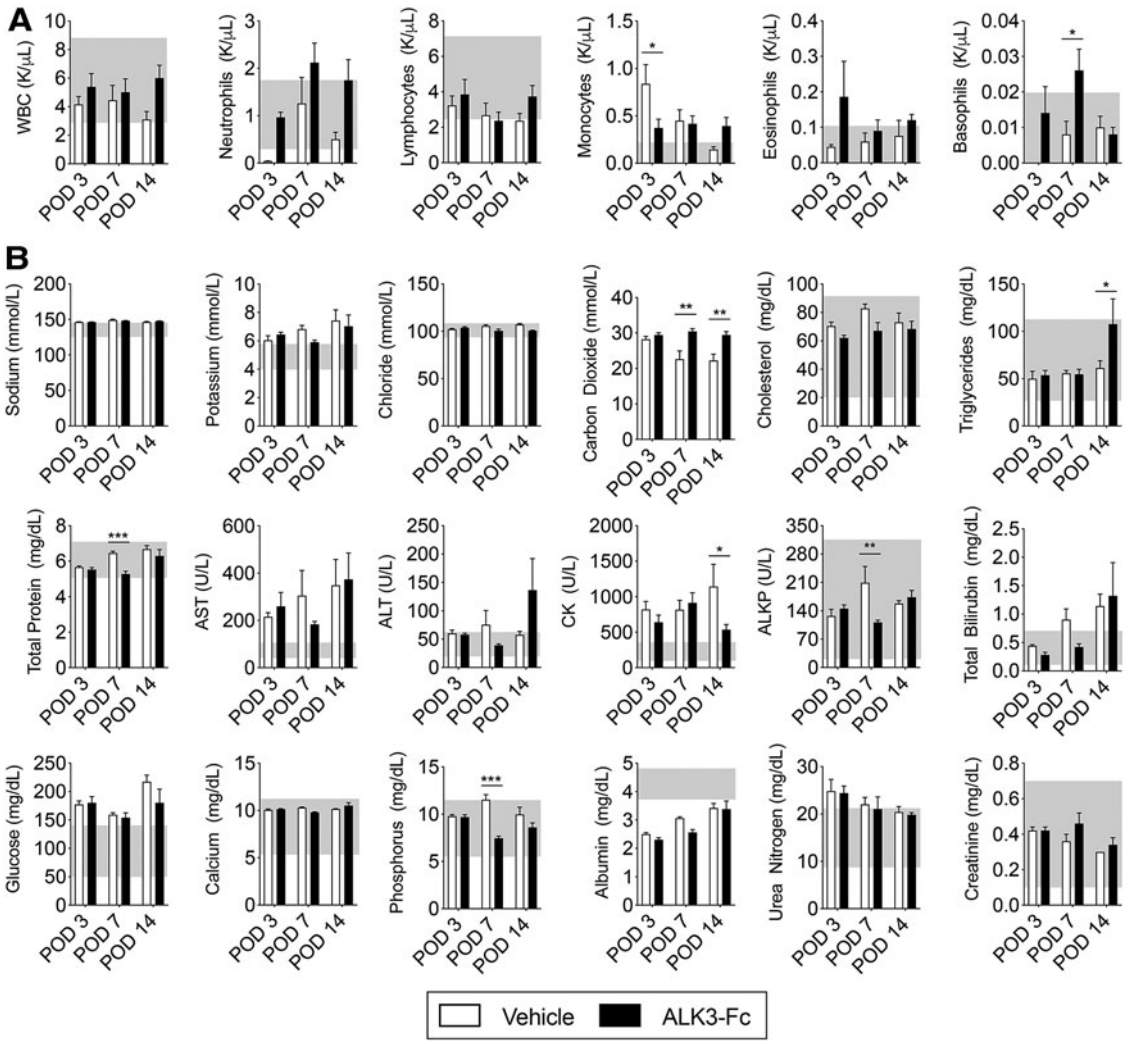

FIG. 3. No systemic side effects following treatment with ALK3-Fc. Following blast-related polytraumatic extremity injury and MRSA infection, rats were treated with vehicle (PBS, $n=3$) or ALK3-Fc (3 mg/kg, $n=3$) twice a week with intraperitoneal injections and whole blood was analyzed on POD3, POD7, and POD14. Blood was collected from the tail vein and immediately subjected to analysis. **(A)** Complete blood count and **(B)** comprehensive metabolic profile were evaluated. Mean ± SEM. $*P<0.05$, $**P<0.01$, comparing vehicle and ALK3-Fc treatment. *Gray box* indicates normal references values. WBC, white blood count; AST, aspartate aminotransferase; ALT, alanine aminotransferase; LDH, lactic acid dehydrogenase; CK, creatine kinase, ALP, alkaline phosphatase.

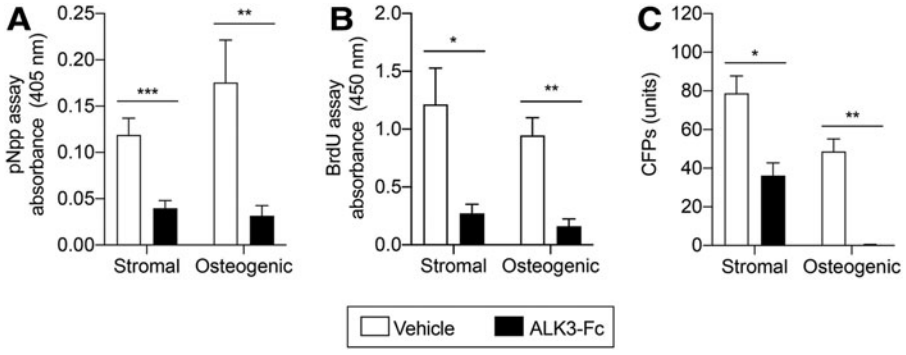

FIG. 4. ALK3-Fc reduces osteogenic differentiation, proliferation, and self-renewal capacity of MPCs. Following blast-related polytraumatic extremity injury and MRSA infection, rats were treated with either vehicle or ALK3-Fc (3 mg/kg) twice a weekly by intraperitoneal injections, and MPCs muscle biopsies at the zone of injury were harvested on POD14 and plated in stromal media or osteogenic media. **(A)** Analysis of early osteogenic differentiation by alkaline phosphatase activity following 6 days in stromal media or ODM. **(B)** Cell proliferation after 6 days in stromal media or ODM and evaluated by BrdU assay. **(C)** Quantification of MPC CFPs by crystal violet after 6 days in stromal media or ODM. Colonies containing >50 cells were counted. Mean ± SEM. $*P<0.05$, $**P<0.01$, $***P<0.001$, comparing vehicle and ALK3-Fc treatment. BrdU, bromodeoxyuridine.

ALK3-Fc augments muscle-like gene expression while inhibiting inflammation following rat blast injury model

To investigate the effects of ALK3-Fc treatment on global gene expression following blast and amputation injury, an unbiased approach was taken and bulk tissue RNA-Seq was performed on muscle-derived tissue harvested from naive uninjured control rats and blast-injured rats on POD14 following vehicle or ALK3-Fc treatment. Based on principal component analysis (PCA) plotting samples according to principal components 1 and 2 (Fig. 5A), expressed genes between naive rats and vehicle-treated rats sampled on POD14 following blast and amputation injury formed two discrete clusters, whereas expressed genes from POD14 ALK3-Fc-treated rats formed an intermediate cluster, with the gene expression in ALK3-Fc-treated rats skewing toward uninjured animals in comparison to the vehicle-treated group. This interpretation of PCA was corroborated further by analysis of differentially expressed genes between these treatment groups and naive animals. Using a standard false discovery rate cutoff ($P < 0.05$), 6,687 genes were differentially expressed in POD14 vehicle-treated rats compared with naive rats, whereas 2,159 genes were differentially expressed in POD14 ALK3-Fc-treated rats compared with naive rats (Fig. 5B). To gain more direct insight into the impact of ALK3-Fc treatment, differential expression was compared between vehicle- and ALK3-Fc-treated rats on POD14, revealing 83 upregulated genes and 203 downregulated genes. Analysis of upregulated genes by pathway and functional analyses using GO terms revealed significant association with biological processes related to muscle development and adaptation, including the term ''muscle structure development'' among the most significant biological processes (Fig. 5C) and with cellular components related to muscle cellular structures (Fig. 5D), suggesting that ALK3-Fc reinforced myogenic gene expression. However, analysis of significantly downregulated genes was associated with biological processes related to immune and inflammation, including the term ''inflammatory response'' among the most significant biological processes, suggesting that ALK3-Fc attenuated these processes (Fig. 5E). A number of genes associated with biological process of muscle structure and development were visualized by a heat map as fold changes compared with naive rats, revealing upregulation of those genes by ALK3-Fc-treatment compared with vehicle treatment on POD14 (Fig. 5F). Similarly, a set of genes associated with biological process of ''inflammatory response'' were visualized by a heat map as fold changes compared with naive rats, revealing repression of those genes by ALK3-Fc compared with vehicle treatment on POD14 (Fig. 5G). Taken together, the results indicate that compared with vehicle treatment, ALK3-Fc activated a transcriptomic signature associated with skeletal muscle structure and development and reduced the expression of genes associated with immune response and inflammation on POD14 following blast and amputation injury.

ALK3-Fc attenuates expression of genes involved in osteogenesis

To gain further insight into the impact of ALK3-Fc treatment on ossification-related pathways with enhanced sensitivity using a candidate-based approach, mRNA expression of a panel of 83 target genes was assayed in tissue harvested from the zone of injury surrounding the amputation site from vehicle- and ALK3-Fc-treated rats on POD3, POD7, and POD14. Gene transcript levels exhibiting a greater than two-fold, statistically significant difference between treatment groups was considered altered. A total of 55 genes were significantly altered on POD3 with the top 5 most decreased genes being *Tac1* (−4.1E4-fold), *Col10a1* (−83.5-fold), *Sox2* (−700.0-fold), *Bglap* (−312.4-fold), and *Smad3* (−172.5-fold; $P < 0.05$; Table 1) in ALK3-Fc- versus vehicle-treated rats. On POD7, 32 genes were altered with the top 5 greatest decreases observed in *Adipoq* (−19.9-fold), *Fgf10* (−6.77-fold), *Sparc* (−6.2-fold), *Adipor1* (−5.8-fold), and *Vegfa* (−5.4-fold) expression ($P < 0.05$; Table 1). A total of 50 genes were altered on POD14 with the top 5 greatest decreases observed in *Tac1* (−1.2E4-fold), *Il6* (−233.7-fold), *Bglap* (−201.4-fold), *Sox2* (−140.1), and *Tert* (−111.1) expression ($P < 0.05$; Table 1). Ontology terms and KEGG pathway analysis were performed with altered genes for each day with Database for Annotation, Visualization and Integrated Discover (DAVID), and alterations in endochondral ossification, BMP/TGF-β-associated SMAD signaling, and osteoblast differentiation were observed (Table 2). These findings suggest that ALK3-Fc treatment inhibits osteogenic differentiation by inhibiting the downstream targets that promote chondrogenesis and osteogenesis following trauma.

FIG. 5. ALK3-Fc treatment enhances muscle-like gene expression while reducing inflammatory genes. RNA-Seq analysis of local wound tissues from rats subjected to blast-related polytraumatic extremity injury and MRSA infection treated with vehicle or ALK3-Fc collected on POD14 and compared with uninjured, naive control rats. **(A)** Principal component analysis reveals clustering of samples by treatment groups based on PC1 and PC2. **(B)** A Venn diagram reveals the number of significantly DE genes from DESeq2 analysis comparing POD14 vehicle- and ALK3-Fc-treated with naive controls. Functional analysis (g:Profiler) by GO terms and adjusted P values (P_{adj}) reveals significantly upregulated genes from DE analysis comparing POD14 vehicle-treated and POD14 ALK3-Fc-treated rats, showing **(C)** the top 20 significant BP and **(D)** the significant CC. **(E)** Functional analysis of g:Profiler functional analysis results showing GO terms and P_{adj} using the list of significantly downregulated genes from the differential expression analysis comparing POD14 vehicle-treated rats with POD14 ALK3-Fc-treated animals, showing the top 20 significant BP. **(F, G)** Heat maps showing the fold change in expression of POD14 vehicle- and ALK3-Fc-treated rats compared with naive controls. **(F)** The set of genes from C were ''intersected'' with the biological process of ''muscle structure development,'' and the functional analysis and relative fold expression versus naive samples depicted by heat map according to a linear scale. **(G)** The set of genes from E were ''intersected'' with the biological process of ''inflammatory response'' and relative expression versus naive samples depicted by heat map according to a linear scale. PC, principal components; DE, differentially expressed; GO, Gene Ontology; BP, biological processes; CC, cellular components.

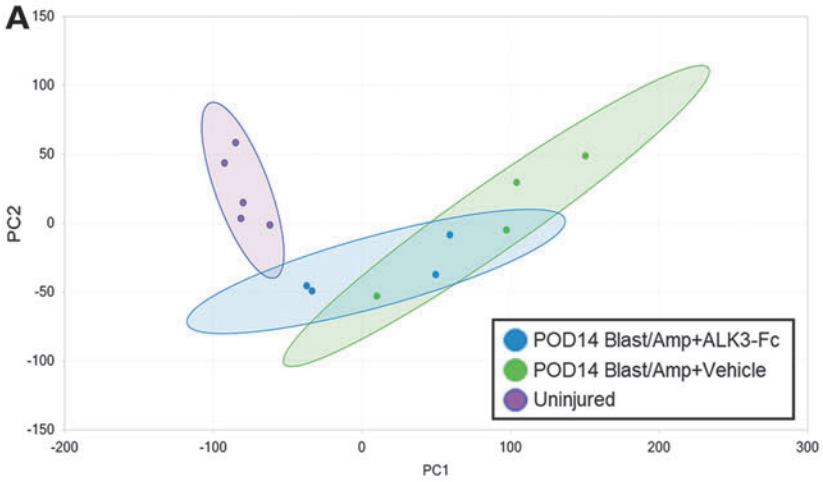

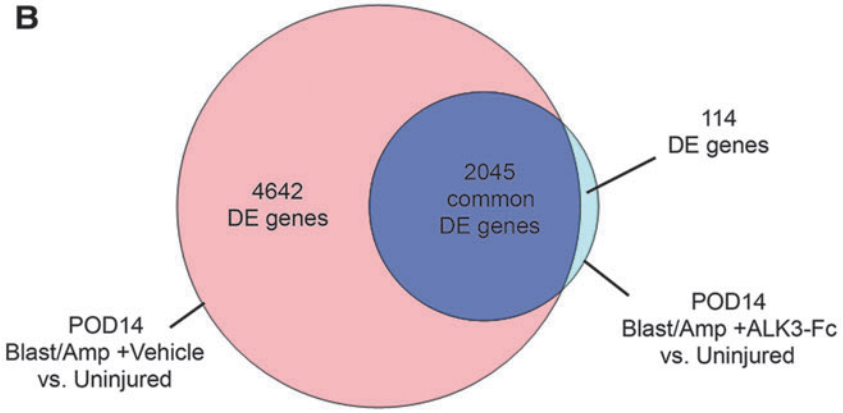

C

GO:BP

term_name	term_id	Padj
muscle organ development	GO:0007517	4.55E-08
muscle structure development	GO:0061061	1.48E-07
skeletal muscle adaptation	GO:0043501	1.50E-06
cardiac muscle tissue morphogenesis	GO:0055008	4.85E-06
muscle tissue morphogenesis	GO:0060415	1.02E-05
muscle organ morphogenesis	GO:0048644	1.52E-05
skeletal muscle organ development	GO:0060538	1.64E-05
striated muscle tissue development	GO:0014706	2.05E-05
transition between fast and slow fiber	GO:0014883	3.10E-05
muscle tissue development	GO:0060537	3.73E-05
muscle system process	GO:0003012	3.83E-05
muscle cell development	GO:0055001	5.57E-05
striated muscle adaptation	GO:0014888	6.05E-05
muscle adaptation	GO:0043500	6.58E-05
skeletal muscle tissue development	GO:0007519	1.52E-04
regulation of muscle system process	GO:0090257	1.57E-04
regulation of skeletal muscle adaptation	GO:0014733	3.05E-04
striated muscle contraction	GO:0006941	5.13E-04
striated muscle cell development	GO:0055002	5.24E-04
slow-twitch skeletal muscle fiber contraction	GO:0031444	9.50E-04

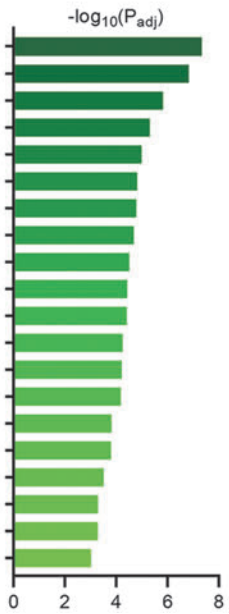

D

GO:BP

term_name	term_id	Padj
sarcomere	GO:0030017	1.39E-08
myofibril	GO:0030016	3.41E-08
contractile fiber	GO:0043292	5.04E-08
I band	GO:0031674	2.39E-06
striated muscle thin filament	GO:0005865	1.99E-04
myofilament	GO:0036379	3.02E-04
actin cytoskeleton	GO:0015629	4.30E-04
supramolecular fiber	GO:0099512	6.12E-04
supramolecular polymer	GO:0099081	6.49E-04
Z disc	GO:0030018	6.78E-04
troponin complex	GO:0005861	3.96E-03
supramolecular complex	GO:0099080	4.26E-03
A band	GO:0031672	1.80E-02
myosin complex	GO:0016459	4.26E-02

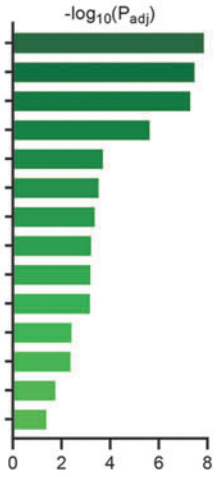

(continued)

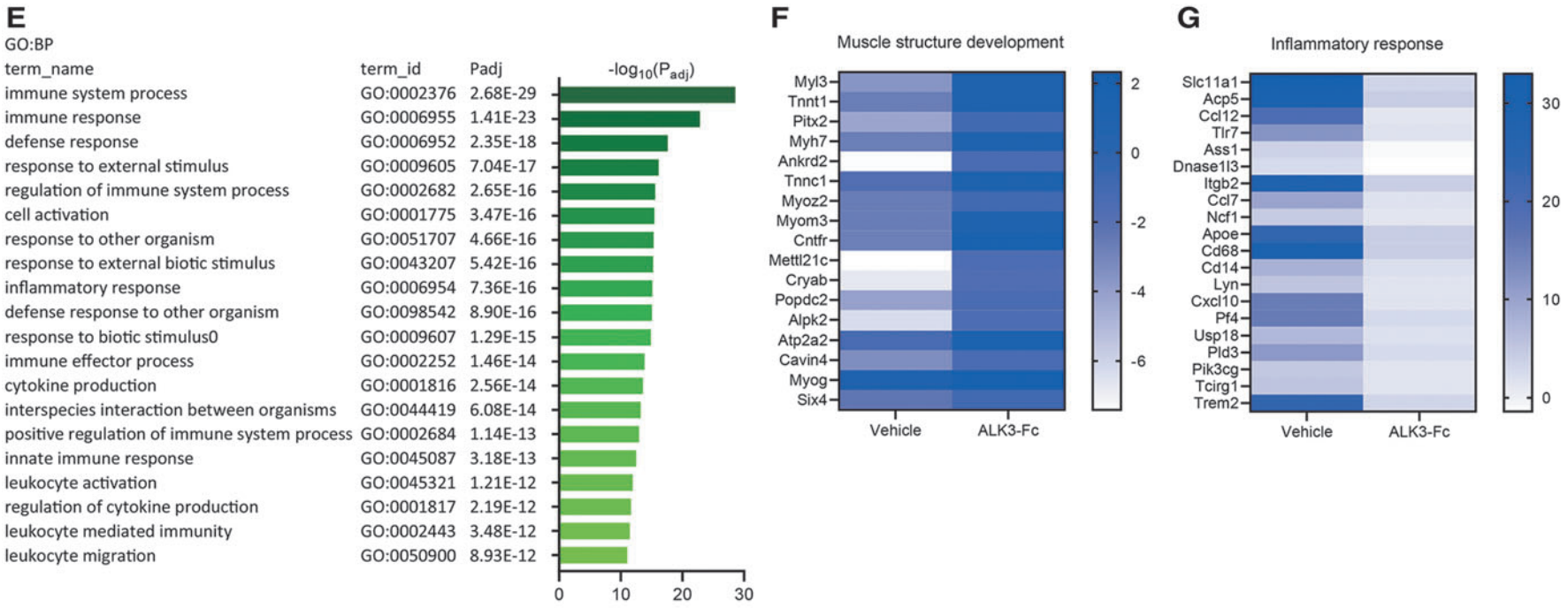

FIG. 5. (Continued).

Table 1. Altered Genes Following ALK3-Fc Treatment in the Rat Blast Injury Model

POD3		*POD7*		*POD14*	
Genes	*Fold change*	*Genes*	*Fold change*	*Genes*	*Fold change*
Tac1	−41722.85	*Adipoq*	−19.95	*Tac1*	−12578.31
Col10a1	−883.56	*Fgf10*	−6.77	*Il6*	−233.75
Sox2	−699.89	*Sparc*	−6.21	*Bglap*	−201.45
Bglap	−312.36	*Adipor1*	−5.77	*Sox2*	−140.09
Smad3	−172.49	*Vegfa*	−5.43	*Tert*	−111.12
Lep	−152.66	*Wnt5a*	−5.41	*Phex*	−91.44
Il6	−102.58	*Igf2*	−5.40	*Il10*	−62.01
Mmp9	−97.29	*Notch1*	−5.14	*Cebpa*	−56.65
Tert	−55.87	*Scarb1*	−5.13	*Smad3*	−46.46
Cxcl1	−49.35	*Lrp5*	−4.96	*Notch1*	−42.37
Runx2	−48.41	*Smurf1*	−4.84	*Fgf2*	−41.74
Tbx5	−36.58	*Fgf1*	−4.78	*Mmp9*	−40.31
Col2a1	−30.07	*Ptk2*	−4.75	*Adipoq*	−38.21
Has1	−28.32	*Itga1*	−4.63	*Ibsp*	−36.01
Phex	−27.61	*Tgfb3*	−4.36	*Smo*	−15.34
Fgf2	−24.31	*Jag1*	−4.32	*Bmp6*	−12.79
Tnf	−20.64	*Cxcl12*	−4.24	*Lep*	−12.37
Cebpa	−16.54	*Sp1*	−4.09	*Smurf1*	−11.59
Pou5f1	−16.16	*Flt1*	−3.98	*Scarb1*	−10.94
Col4a3	−13.72	*Pdgfa*	−3.85	*Tnf*	−10.27
Smo	−11.97	*Myod1*	−3.65	*Col4a3*	−8.39
Notch1	−11.38	*Smurf2*	−3.51	*Sox9*	−8.15
Il10	−10.10	*Fgf2*	−3.48	*Alpl*	−8.02
Bmp2	−9.49	*Angpt2*	−3.29	*Eng*	−7.42
Bmp6	−7.20	*Itgav*	−3.00	*Fgf1*	−3.91
Alpl	−5.14	*Bmp6*	−2.91	*Has2*	−3.48
Cxcl10	−4.77	*Ptch1*	−2.87	*Fgf10*	−3.33
Fgf10	−3.30	*Col4a3*	−2.84	*Sp1*	−3.08
Smurf1	−2.95	*Kdr*	−2.75	*Itga1*	−2.71
Tgfb3	3.71	*Rhoa*	−2.58	*Comp*	2.07
Ptch1	4.12	*Hat1*	−2.55	*Angpt2*	4.22
Itga2	6.73	*Pou5f1*	4.52	*Omd*	4.36
Ptk2	7.96			*Myod1*	5.22
Omd	8.40			*Lrp5*	5.73
Pdgfa	8.85			*Cd44*	5.81
Hat1	11.16			*Tgfb1*	5.94
Tgfb1	14.39			*Ccl2*	7.86
Adipor1	14.40			*Pdgfa*	8.51
Cd44	15.79			*Vegfa*	15.30
Bmp4	24.49			*Bmp4*	15.56
Sparc	26.68			*Hdac1*	15.66
Comp	34.44			*Smurf2*	15.90
Angpt2	37.33			*Jag1*	19.17
Smurf2	66.71			*Flt1*	23.32
Hdac1	73.24			*Sparc*	30.91
Jag1	76.74			*Gusb*	47.09
Myod1	92.58			*Itgav*	57.60
Itgav	97.71			*Col1a1*	112.98
Vegfa	100.37			*Fabp4*	251.24
Flt1	110.52			*Kdr*	374.42
Lrp5	142.38				
Gusb	153.83				
Fabp4	196.00				
Itgam	512.00				
Col1a1	808.03				

POD, postoperative day.

Discussion

tHO is a common event following musculoskeletal injury sustained in modern combat and leads to significant impairment in daily function [38]. Given the complications associated with tHO, there is a need to develop novel therapeutic options to limit the devastating disease. In the current study, rats subjected to a blast-related polytraumatic extremity injury and MRSA wound infection were treated with kinase inhibitors LDN193189 and LDN212854 or

Table 2. Top Regulated Terms from Gene Ontology Domains and KEGG Pathway Analysis from POD3, POD7, and POD14

ID	*Name*	*Concept*	*No. of genes*	*FDR*
POD3				
GO:0001958	Endochondral ossification	GOBP	5	6.30E-04
GO:0060395	SMAD protein signal transduction	GOBP	6	1.79E-03
GO:0000122	Negative regulation of transcription from RNA polymerase II promoter	GOBP	10	5.86E-03
GO:0045944	Positive regulation of transcription from RNA polymerase II promoter	GOBP	11	1.12E-02
GO:0045669	Positive regulation of osteoblast differentiation	GOBP	5	1.35E-02
GO:0007155	Cell adhesion	GOBP	7	1.64E-02
GO:0043408	Regulation of MAPK cascade	GOBP	5	2.39E-02
GO:0010862	Positive regulation of pathway-restricted SMAD protein phosphorylation	GOBP	5	2.66E-02
GO:0048468	Cell development	GOBP	5	3.26E-02
GO:0051897	Positive regulation of protein kinase B signaling	GOBP	5	3.26E-02
GO:0005615	Extracellular space	GOCC	21	8.35E-10
GO:0005576	Extracellular region	GOCC	11	2.13E-03
GO:0005125	Cytokine activity	GOMF	8	4.75E-04
GO:0008201	Heparin binding	GOMF	6	2.13E-02
ssc05200	Pathways in cancer	KEGG	16	2.05E-07
ssc05205	Proteoglycans in cancer	KEGG	10	3.74E-04
ssc04350	TGF-beta signaling pathway	KEGG	7	2.47E-03
ssc05144	Malaria	KEGG	6	6.67E-03
ssc05321	Inflammatory bowel disease	KEGG	6	1.48E-02
ssc04151	PI3K-Akt signaling pathway	KEGG	10	3.22E-02
ssc05410	HCM	KEGG	6	4.92E-02
POD7				
GO:0001938	Positive regulation of endothelial cell proliferation	GOBP	5	2.73E-03
GO:0045944	Positive regulation of transcription from RNA polymerase II promoter	GOBP	9	1.03E-02
GO:0030154	Cell differentiation	GOBP	6	1.51E-02
GO:0010595	Positive regulation of endothelial cell migration	GOBP	4	2.56E-02
GO:0045766	Positive regulation of angiogenesis	GOBP	5	2.83E-02
GO:0051781	Positive regulation of cell division	GOBP	4	3.88E-02
GO:0008201	Heparin binding	GOMF	6	9.44E-04
ssc05200	Pathways in cancer	KEGG	12	4.65E-05
ssc04015	Rap1 signaling pathway	KEGG	9	5.25E-04
ssc04014	Ras signaling pathway	KEGG	9	8.68E-04
ssc04151	PI3K-Akt signaling pathway	KEGG	10	1.54E-03
ssc05205	Proteoglycans in cancer	KEGG	8	4.46E-03
POD14				
GO:0045944	Positive regulation of transcription from RNA polymerase II promoter	GOBP	13	3.85E-05
GO:0001649	Osteoblast differentiation	GOBP	6	3.16E-03
GO:0014068	Positive regulation of phosphatidylinositol 3-kinase signaling	GOBP	5	1.68E-02
GO:0001525	Angiogenesis	GOBP	6	3.16E-02
GO:0005615	Extracellular space	GOCC	20	8.65E-10
GO:0005576	Extracellular region	GOCC	10	6.70E-03
GO:0008083	Growth factor activity	GOMF	5	3.01E-02
GO:0005125	Cytokine activity	GOMF	6	6.09E-02
ssc04151	PI3K-Akt signaling pathway	KEGG	14	3.81E-06
ssc05200	Pathways in cancer	KEGG	14	2.76E-05
ssc05205	Proteoglycans in cancer	KEGG	10	3.76E-04
ssc04510	Focal adhesion	KEGG	9	5.13E-03
ssc05144	Malaria	KEGG	6	6.70E-03
ssc04350	TGF-beta signaling pathway	KEGG	6	4.64E-02
ssc05410	HCM	KEGG	6	4.94E-02

Altered genes were evaluated by Database for Annotation, Visualization, and Integrated Discover (DAVID).

KEGG, Kyoto Encyclopedia of Genes and Genomes; FDR, false discover rate; GO, gene ontology; GOBP, gene otology biological processes; GOMF, gene otology molecular functions; GOCC, gene otology cellular compartments; HCM, hypertrophic cardiomyopathy; TGF, transforming growth factor.

BMP ligand trap ALK3-Fc to determine the effects on heterotopic bone formation. Rats treated with LDN193189 and LDN212854 exhibited reduced HO formation but developed significant adverse effects at the exposures used. Our group previously reported severe neutropenia and reduced macrophage infiltration following treatment with LDN193189 in the mouse burn/tenotomy model of HO [15]. The potential immunosuppressive effects of LDN193189 might explain the metastatic MRSA lesions that were observed in some animals within two postoperative weeks of

treatment. While LDN193189 is a potent, low nanomolar inhibitor of ALK2 and ALK3 signaling, it also exhibits TGF-β receptor inhibition at concentrations of >500 nM, as well as inhibition of RIPK2, ABL, and SRC kinase pathways, potentially eliciting antifibrotic and anti-inflammatory effects that could enhance the efficacy but could also lead to adverse effects [15,39] by exerting immunomodulatory effects that would be detrimental in the context of bacteremia and low-grade sepsis. While rats have been previously subjected to similar or higher exposures of LDN193189 in other studies without apparent toxicity [40], the combination of treatment, polytrauma, and MRSA exposure in this model might have revealed novel adverse effects. It is not clear if lower exposures to these kinase inhibitors, or the use of more selective ALK2/ALK3 inhibitor molecules, would be as effective or better tolerated. In contrast, ALK3-Fc did not elicit systemic side effects for the duration of the observational study (12 weeks). ALK3-Fc targets primarily BMP2 and BMP4, whereas LDN193189 and LDN212854 blocks signaling via these ligands as well as a multitude of other ligands including BMP6 and BMP7. Together, these results suggest that ALK3-Fc has an improved therapeutic index compared with the first-generation kinase inhibitors in this model due to reduced secondary side effects.

We have shown the important role of BMP signaling in two distinct models of traumatic HO, a burn/tenotomy model [15] and a systemic blast-associated lower limb amputation model, incorporating multiple orthopedic injuries and wound infection. HO formed in both these models shares strong similarities as previously published [14,33], which formed the basis of testing the impact of targeting multiple BMP receptors and ligands in inhibiting this complex post-traumatic pathology. LDN193189 and LDN212854 have been previously reported to inhibit HO in the rare genetic disorder fibrodysplasia ossificans progressiva (FOP), where ectopic ossification is driven by a gain-of-function mutation in *ACVR1* expressing ALK2 [27,30,41,42]. Results from the current study are consistent with findings from the genetic model, highlighting a critical role of ALK2/ALK3 and their associated BMP ligands targeted by these compounds in the development of HO in both congenital and acquired forms of HO. It is interesting to note that the studies of LDN193189 in the FOP mouse models did not report any of the adverse effects observed in our study of traumatic HO. The complex tHO model in this study was associated a greater degree of tissue injury, wound healing, and infection, and these factors may have contributed to the adverse effects observed in tHO models and may have revealed dose-limiting toxicities associated with these first-generation BMP type I receptor kinase inhibitors. However, the mechanistic process of ectopic endochondral bone formation in skeletal muscle and soft tissue in our blast-related polytraumatic injury model is consistent with the cellular, molecular, clinical, and radiographic features observed in patients leading to maturation of bone tissue [32]. Classically, the HO that forms in patients is not connected to the periosteum but has the potential to later fuse with the periosteum of the bone as a secondary feature [43]. The significant weight loss and sporadic development of metastatic lesions with evidence of systemic infection with the LDN193189 probe compound in the rat tHO model would suggest the need for a cautious approach, particularly due to its similarities to human HO, and the need to test distinct chemotypes to determine if these effects are on-target or off-target, and potentially surmounted using more selective kinase inhibitor compounds.

In our gene expression analysis, the impact on ALK3-Fc in suppressing expression of genes associated with endochondral ossification and SMAD-dependent signaling was not unanticipated; however, several pathways associated with myogenesis, angiogenesis, and inflammation were also shown to be modulated by treatment with ALK3-Fc, using RNA-Seq profiling as well as the analysis of expression of a curated panel of relevant genes. BMPs have previously been found to influence vascular cell proliferation, to increase endothelial cell adhesiveness to circulating inflammatory cells in a reactive oxygen species (ROS)-dependent manner, and to modulate the inflammatory response [44,45]. Specifically, BMPs have been shown to act synergistically with vascular endothelial growth factor (VEGF) to enhance cell survival, cartilage formation, and mineralized bone formation [46]. Both VEGF and interleukin (IL)-6 have potent pro-angiogenic activity [47]. Others have shown that IL-6 is an important regulator of angiogenesis wherein VEGF concentrations tend to correlate with IL-6-increased VEGF levels [48]. VEGF has also been show to increase vascular permeability after promoting local angiogenesis and facilitating the recruitment of MPCs to indirectly enhance bone formation [49]. Thus, inhibiting VEGF has previously been shown to not only reduce angiogenesis but also result in reduced osteogenesis [50]. HO lesions have been shown to be highly vascular, and VEGF produced by MPCs plays a critical role in ectopic bone formation, whereby inhibition of these signals significantly reduces HO formation [51]. In our analysis, we also found reduced VEGF and IL-6 expression following ALK3-Fc. These findings would suggest that there is a potential synergistic effect of BMPs and VEGF in limiting tHO; however, additional analyses are certainly necessary to confirm these findings.

Conclusion

The current study demonstrates that broader BMP type I receptor kinase inhibition and more selective BMP ligand trap treatments may be effective at inhibiting tHO; however, additional analyses are necessary to elucidate the precise identity of the BMP ligands that mediate the recruitment and proliferation of MPC and other cells that initiate inflammation, osteogenic differentiation, and wound healing contributing to HO formation. While LDN193189 and LDN212854 were more potent at limiting the development of tHO, the systemic adverse effects observed would need to be overcome with more optimal dosing or by using more selective agents. It is unclear if the limited tolerability is due to an on-target effect from broad suppression of the BMP signaling pathway or the many well-known off-target effects of these first-generation BMP type I receptor kinase inhibitor probes [39]. Additional studies using more selective and clinically translatable small molecules are necessary. The ligand trap ALK3-Fc affects a smaller subset of BMP ligands and had less potent effects on tHO, but ALK3-Fc was more tolerable and represented a more immediately translatable approach for targeting the complex tHO in this current model.

Disclaimer

The opinions or assertions contained herein are the private ones of the authors and are not to be construed as official or reflecting the views of the Department of Defense, the

Uniformed Services University of the Health Sciences, or any other agency of the United States Government.

Financial Disclosures

P.B.Y. is a co-founder and holds stock in Keros Therapeutics, which develops therapies for hematologic and musculoskeletal diseases targeting BMP and TGFβ signaling pathways. P.B.Y. interests are reviewed and managed by Brigham and Women's Hospital in accordance with their conflict of interest policies. The remaining authors have no financial disclosures.

Author Disclosure Statement

No competing financial interests exist.

Funding Information

This work was supported by funding from the National Institute of Health/National Institute of Arthritis and Musculoskeletal and Skin Diseases NIH R01-AR071379 and R01-GM123069 (B.L.), NIH R01-AR057374, and UG3-TR002617 (P.B.Y.), the American College of Surgeons Clowes Award (B.L.), the International Fibrodysplasia Ossificans Progressiva Research Awards (B.L. and P.B.Y.), and Congressionally Directed Medical Research Program grant (W81XWH-16-2-0051) (T.A.D. and M.J.B. with subawards to B.L. and P.B.Y.).

References

1. Alfieri KA, JA Forsberg and BK Potter. (2012). Blast injuries and heterotopic ossification. Bone Joint Res 1:192–197.
2. Potter BK, TC Burns, AP Lacap, RR Granville and D Gajewski. (2006). Heterotopic ossification in the residual limbs of traumatic and combat-related amputees. J Am Acad Orthop Surg 14:S191–S197.
3. Potter BK, TC Burns, AP Lacap, RR Granville and DA Gajewski. (2007). Heterotopic ossification following traumatic and combat-related amputations. Prevalence, risk factors, and preliminary results of excision. J Bone Joint Surg Am 89:476–486.
4. Melcer T, B Belnap, GJ Walker, P Konoske and M Galarneau. (2011). Heterotopic ossification in combat amputees from Afghanistan and Iraq wars: five case histories and results from a small series of patients. J Rehabil Res Dev 48:1–12.
5. Pittenger MF, AM Mackay, SC Beck, RK Jaiswal, R Douglas, JD Mosca, MA Moorman, DW Simonetti, S Craig and DR Marshak. (1999). Multilineage potential of adult human mesenchymal stem cells. Science 284:143–147.
6. Beederman M, JD Lamplot, G Nan, J Wang, X Liu, L Yin, R Li, W Shui, H Zhang, et al. (2013). BMP signaling in mesenchymal stem cell differentiation and bone formation. J Biomed Sci Eng 6:32–52.
7. Wu M, G Chen and YP Li. (2016). TGF-β and BMP signaling in osteoblast, skeletal development, and bone formation, homeostasis and disease. Bone Res 4:16009.
8. Chen D, M Zhao and GR Mundy. (2004). Bone morphogenetic proteins. Growth Factors 22:233–241.
9. Luu HH, WX Song, X Luo, D Manning, J Luo, ZL Deng, KA Sharff, AG Montag, RC Haydon and TC He. (2007). Distinct roles of bone morphogenetic proteins in osteogenic differentiation of mesenchymal stem cells. J Orthop Res 25:665–677.
10. Katagiri T, S Tsukamoto and M Kuratani. (2018). Heterotopic bone induction via BMP signaling: potential therapeutic targets for fibrodysplasia ossificans progressiva. Bone 109:241–250.
11. Dey D, BM Wheatley, D Cholok, S Agarwal, PB Yu, B Levi and TA Davis. (2017). The traumatic bone: trauma-induced heterotopic ossification. Transl Res 186:95–111.
12. Noël D, D Gazit, C Bouquet, F Apparailly, C Bony, P Plence, V Millet, G Turgeman, M Perricaudet, J Sany and C Jorgensen. (2004). Short-term BMP-2 expression is sufficient for in vivo osteochondral differentiation of mesenchymal stem cells. Stem Cells 22:74–85.
13. Shu B, M Zhang, R Xie, M Wang, H Jin, W Hou, D Tang, SE Harris, Y Mishina, et al. (2011). BMP2, but not BMP4, is crucial for chondrocyte proliferation and maturation during endochondral bone development. J Cell Sci 124:3428.
14. Peterson JR, S De La Rosa, O Eboda, KE Cilwa, S Agarwal, SR Buchman, PS Cederna, C Xi, MD Morris, et al. (2014). Treatment of heterotopic ossification through remote ATP hydrolysis. Sci Transl Med 6:255ra132.
15. Agarwal S, SJ Loder, C Breuler, J Li, D Cholok, C Brownley, J Peterson, HH Hsieh, J Drake, et al. (2017). Strategic targeting of multiple BMP receptors prevents trauma-induced heterotopic ossification. Mol Ther 25:1974–1987.
16. Kang H, AB Dang, SK Joshi, B Halloran, R Nissenson, X Zhang, J Li, HT Kim and X Liu. (2014). Novel mouse model of spinal cord injury-induced heterotopic ossification. J Rehabil Res Dev 51:1109–1118.
17. Li L, Y Jiang, H Lin, H Shen, J Sohn, PG Alexander and RS Tuan. (2019). Muscle injury promotes heterotopic ossification by stimulating local bone morphogenetic protein-7 production. J Orthop Transl 18:142–153.
18. Shen B, A Wei, S Whittaker, LA Williams, H Tao, DD Ma and AD Diwan. (2010). The role of BMP-7 in chondrogenic and osteogenic differentiation of human bone marrow multipotent mesenchymal stromal cells in vitro. J Cell Biochem 109:406–416.
19. Miyazono K, S Maeda and T Imamura. (2005). BMP receptor signaling: transcriptional targets, regulation of signals, and signaling cross-talk. Cytokine Growth Factor Rev 16:251–263.
20. Sieber C, J Kopf, C Hiepen and P Knaus. (2009). Recent advances in BMP receptor signaling. Cytokine Growth Factor Rev 20:343–355.
21. Luo J, M Tang, J Huang, BC He, JL Gao, L Chen, GW Zuo, W Zhang, Q Luo, et al. (2010). TGFbeta/BMP type I receptors ALK1 and ALK2 are essential for BMP9-induced osteogenic signaling in mesenchymal stem cells. J Biol Chem 285:29588–29598.
22. Liu H, R Zhang, D Chen, BO Oyajobi and M Zhao. (2012). Functional redundancy of type II BMP receptor and type IIB activin receptor in BMP2-induced osteoblast differentiation. J Cell Physiol 227:952–963.
23. Gamer LW, K Tsuji, K Cox, LP Capelo, J Lowery, H Beppu and V Rosen. (2011). BMPR-II is dispensable for formation of the limb skeleton. Genesis 49:719–724.
24. Bragdon B, O Moseychuk, S Saldanha, D King, J Julian and A Nohe. (2011). Bone morphogenetic proteins: a critical review. Cell Signal 23:609–620.
25. Schmierer B and CS Hill. (2007). TGFbeta-SMAD signal transduction: molecular specificity and functional flexibility. Nat Rev Mol Cell Biol 8:970–982.
26. Hong CC and PB Yu. (2009). Applications of small molecule BMP inhibitors in physiology and disease. Cytokine Growth Factor Rev 20:409–418.

27. Yu PB, DY Deng, CS Lai, CC Hong, GD Cuny, ML Bouxsein, DW Hong, PM McManus, T Katagiri, et al. (2008). BMP type I receptor inhibition reduces heterotopic [corrected] ossification. Nat Med 14:1363–1369.
28. Mohedas AH, X Xing, KA Armstrong, AN Bullock, GD Cuny and PB Yu. (2013). Development of an ALK2-biased BMP type I receptor kinase inhibitor. ACS Chem Biol 8:1291–1302.
29. Derwall M, R Malhotra, CS Lai, Y Beppu, E Aikawa, JS Seehra, WM Zapol, KD Bloch and PB Yu. (2012). Inhibition of bone morphogenetic protein signaling reduces vascular calcification and atherosclerosis. Arterioscler Thromb Vasc Biol 32:613–622.
30. Cuny GD, PB Yu, JK Laha, X Xing, J-F Liu, CS Lai, DY Deng, C Sachidanandan, KD Bloch and RT Peterson. (2008). Structure-activity relationship study of bone morphogenetic protein (BMP) signaling inhibitors. Bioorg Med Chem Lett 18:4388–4392.
31. Greenblatt MB, JH Shim and LH Glimcher. (2010). TAK1 mediates BMP signaling in cartilage. Ann N Y Acad Sci 1192:385–390.
32. Qureshi AT, D Dey, EM Sanders, JG Seavey, AM Tomasino, K Moss, B Wheatley, D Cholok, S Loder, et al. (2017). Inhibition of mammalian target of rapamycin signaling with rapamycin prevents trauma-induced heterotopic ossification. Am J Pathol 187:2536–2545.
33. Qureshi AT, EK Crump, GJ Pavey, DN Hope, JA Forsberg and TA Davis. (2015). Early characterization of blast-related heterotopic ossification in a rat model. Clin Orthop Relat Res 473:2831–2839.
34. Pavey GJ, AT Qureshi, DN Hope, RL Pavlicek, BK Potter, JA Forsberg and TA Davis. (2015). Bioburden increases heterotopic ossification formation in an established rat model. Clin Orthop Relat Res 473:2840–2847.
35. Love MI, W Huber and S Anders. (2014). Moderated estimation of fold change and dispersion for RNA-seq data with DESeq2. Genome Biol 15:550.
36. Raudvere U, L Kolberg, I Kuzmin, T Arak, P Adler, H Peterson and J Vilo. (2019). g:Profiler: a web server for functional enrichment analysis and conversions of gene lists (2019 update). Nucleic Acids Res 47:W191–W198.
37. Huang da W, BT Sherman and RA Lempicki. (2009). Systematic and integrative analysis of large gene lists using DAVID bioinformatics resources. Nat Protoc 4:44–57.
38. Daniels CM, GJ Pavey, J Arthur, M Noller, JA Forsberg and BK Potter. (2018). Has the proportion of combat-related amputations that develop heterotopic ossification increased? J Orthop Trauma 32:283–287.
39. Vogt J, R Traynor and GP Sapkota. (2011). The specificities of small molecule inhibitors of the TGFß and BMP pathways. Cell Signal 23:1831–1842.
40. Theurl I, A Schroll, T Sonnweber, M Nairz, M Theurl, W Willenbacher, K Eller, D Wolf, M Seifert, et al. (2011). Pharmacologic inhibition of hepcidin expression reverses anemia of chronic inflammation in rats. Blood 118:4977–4984.
41. Culbert AL, SA Chakkalakal, EG Theosmy, TA Brennan, FS Kaplan and EM Shore. (2014). Alk2 regulates early chondrogenic fate in fibrodysplasia ossificans progressiva heterotopic endochondral ossification. Stem Cells 32:1289–1300.
42. Hwang C, CA Pagani, N Das, S Marini, AK Huber, L Xie, J Jimenez, S Brydges, WK Lim, et al. (2020). Activin A does not drive post-traumatic heterotopic ossification. Bone 138:115473.
43. Meyers C, J Lisiecki, S Miller, A Levin, L Fayad, C Ding, T Sono, E McCarthy, B Levi and AW James. (2019). Heterotopic ossification: a comprehensive review. JBMR Plus 3:e10172.
44. Sorescu GP, H Song, SL Tressel, J Hwang, S Dikalov, DA Smith, NL Boyd, MO Platt, B Lassègue, KK Griendling and H Jo. (2004). Bone morphogenic protein 4 produced in endothelial cells by oscillatory shear stress induces monocyte adhesion by stimulating reactive oxygen species production from a nox1-based NADPH oxidase. Circ Res 95:773–779.
45. Csiszar A, N Labinskyy, H Jo, P Ballabh and Z Ungvari. (2008). Differential proinflammatory and prooxidant effects of bone morphogenetic protein-4 in coronary and pulmonary arterial endothelial cells. Am J Physiol Heart Circ Physiol 295:H569–H577.
46. Peng H, V Wright, A Usas, B Gearhart, H-C Shen, J Cummins and J Huard. (2002). Synergistic enhancement of bone formation and healing by stem cell-expressed VEGF and bone morphogenetic protein-4. J Clin Invest 110:751–759.
47. Tzeng HE, CH Tsai, ZL Chang, CM Su, SW Wang, WL Hwang and CH Tang. (2013). Interleukin-6 induces vascular endothelial growth factor expression and promotes angiogenesis through apoptosis signal-regulating kinase 1 in human osteosarcoma. Biochem Pharmacol 85: 531–540.
48. Huang Y-H, H-Y Yang, S-W Huang, G Ou, Y-F Hsu and M-J Hsu. (2016). Interleukin-6 induces vascular endothelial growth factor-C expression via Src-FAK-STAT3 signaling in lymphatic endothelial cells. PLoS One 11:e0158839.
49. Kempen DHR, L Lu, A Heijink, TE Hefferan, LB Creemers, A Maran, MJ Yaszemski and WJA Dhert. (2009). Effect of local sequential VEGF and BMP-2 delivery on ectopic and orthotopic bone regeneration. Biomaterials 30:2816–2825.
50. Peng H, A Usas, A Olshanski, AM Ho, B Gearhart, GM Cooper and J Huard. (2005). VEGF improves, whereas sFlt1 inhibits, BMP2-induced bone formation and bone healing through modulation of angiogenesis. J Bone Miner Res 20:2017–2027.
51. Hwang C, S Marini, AK Huber, DM Stepien, M Sorkin, S Loder, CA Pagani, J Li, ND Visser, et al. (2019). Mesenchymal VEGFA induces aberrant differentiation in heterotopic ossification. Bone Res 7:36.

Address correspondence to:
Dr. Thomas A. Davis
Department of Surgery
Uniformed Services University
of the Health Sciences
4301 Jones Bridge Road
Bethesda, MD 20814
USA

E-mail: thomas.davis@usuhs.edu

Dr. Benjamin Levi
Division of Plastic Surgery
Department of Surgery
University of Michigan Health Systems
1500 East Medical Center Drive
Ann Arbor, MI 48109-0340
USA

E-mail: blevi@med.umich.edu

Received for publication September 25, 2020
Accepted after revision November 25, 2020
Prepublished on Liebert Instant Online November 30, 2020